Phase-frequency model of strongly pulse-coupled Belousov-Zhabotinsky oscillators

Viktor Horváth (iD), Daniel Jackson Kutner, Manhao Danny Zeng, and Irving R. Epstein (iD)

View Online   Export Citation   CrossMark

Phase-frequency model of strongly pulse-coupled Belousov-Zhabotinsky oscillators

View Online   Export Citation   CrossMark

Viktor Horváth,[1] [ID] Daniel Jackson Kutner,[2] Manhao Danny Zeng,[3] and Irving R. Epstein[1,a) [ID]

AFFILIATIONS

[1] Department of Chemistry, Brandeis University, MS 015, Waltham, Massachusetts 02454-9110, USA
[2] Department of Physics, University of California, Santa Barbara, California 93106-9530, USA
[3] Department of Chemistry and Biochemistry, University of California, Santa Barbara, California 93106-9510, USA

Note: This paper is part of the Focus Issue, "Nonlinear Chemical Dynamics and Its Interdisciplinary Impact: Dedicated to Ken Showalter on the Occasion of his 70th Birthday".
[a)]**Electronic mail:** epstein@brandeis.edu

ABSTRACT

We demonstrate that the dynamical behavior of strongly pulse-coupled Belousov-Zhabotinsky oscillators can be reproduced and predicted using a model that treats both the phase and the instantaneous frequency of the oscillators. Model parameters are extracted from the experimental data obtained using a single pulse-perturbed oscillator and are used to simulate the temporal dynamics of a system of two coupled oscillators. Our model exhibits the out-of-phase and anti-phase synchronization and the 1:N and N:M temporal patterns as well as the oscillator suppression that are observed in experiments when the inhibitory coupling is asymmetric. This approach may be adapted to other systems, such as coupled neurons, where the oscillatory dynamics is affected by strong pulses.

One of the most frequently used approaches to modeling the dynamics of coupled oscillators involves reduction of the periodic behavior of a single oscillator to a single time dependent periodic function (phase) and a function describing the interaction between oscillators (phase response curve). While such a treatment can yield elegant and appealing mathematical results and allows for treating systems comprising hundreds or thousands of oscillators, it treats them as rigid clocks, which is inadequate in many cases, including chemical oscillators. Here, we present an experimental example of such a system and demonstrate that by introducing a second time-dependent variable (frequency), the behaviors that a pair of pulse-coupled Belousov-Zhabotinsky oscillators display can be adequately reproduced and predicted using parameters extracted from experiments on a single oscillator. Our approach may be applied to model other systems, where long-term adaptation of individual oscillators occurs, such as coupled neurons.

I. INTRODUCTION

Among his many contributions to nonlinear science, Showalter has done groundbreaking work on elucidating the behavior of coupled chemical oscillators. Three decades ago, he pioneered the use of beads of ferroin-loaded cation-exchange resin as a medium for generating and studying novel spatiotemporal patterns in the Belousov-Zhabotinsky (BZ) reaction.[1] He later utilized this technique to create a chemical analog of the phenomenon known in biology as quorum sensing.[2] More recently, he has explored phase clusters[3] and chimera states[4] in these systems, which consist of large numbers of coupled BZ oscillators. Here, we present an approach to analyzing the behavior of coupled oscillators, drawing on the BZ reaction as our inspiration and source of experimental data.

Pulse-coupled oscillators represent a special class of coupled systems, in which the interactions between oscillators are limited to brief time periods (pulses). A well-known

example is the nervous system, where neurons interact by means of short electrical pulses (action potentials) and pulsatile release of neurotransmitters.[5] Theoretical investigations of pulse-coupled oscillators commonly employ simple phase models, in which oscillators are represented by their phases, and the interactions between oscillators are characterized by phase response curves (PRCs),[6] which measure the phase change as a function of the phase of perturbation. This simple but powerful approach has been used to explain common synchronization phenomena such as in-phase[7,8] and out-of-phase[9] oscillations, bursting,[10] oscillator death,[11] and dynamical clustering in networks of neurons[12] as well as some system-specific behaviors such as alternating firing order.[13]

Phase models[14–17] were first employed to investigate synchronization in large sets of weakly coupled oscillators. Their applicability to pulse-coupled oscillators rests on the assumption that the coupling is sufficiently weak that each oscillator returns to its original unperturbed limit cycle after completing the cycle during which the pulse is received; i.e., the oscillator quickly "forgets" the perturbation.

When the coupling is strong, as in chemical or neural oscillators, this assumption may be violated:[18,19] the oscillatory dynamics is altered such that the unperturbed cycles are different before and after the perturbed cycle. Thus, the oscillators are not memory-less,[6] which may bring about more complex collective behaviors.

Inhibitory coupling has been shown to produce in-phase (IP), out-of-phase (OP), and oscillatory-suppressed (OS) modes with two coupled phase oscillators.[9] In addition to this, we observed complex temporal patterns (1:N, N:M, where P:Q signifies that each cycle contains P peaks of one oscillator and Q of the other) in an experimental system comprised of two pulse-coupled Belousov-Zhabotinsky (BZ) oscillators with asymmetric inhibitory coupling, that is, when the coupling strengths are not equal. We attributed the emergence of the complex patterns to long-lasting changes in the chemical composition (memory).[20]

Here, we present an augmented phase-frequency model that can reproduce the observed long-term effect of inhibitory pulse-perturbations in a single BZ oscillator as well as the complex dynamics seen when two BZ oscillators are coupled via unequal inhibitory pulses.

II. EXPERIMENTAL

A single pulse-perturbed BZ oscillator[20] is constructed as follows: Two reagent solutions ($0.4 \, mol/l \, NaBrO_3 + 0.5 \, mol/l \, H_2SO_4$ and $0.1 \, mol/l$ malonic acid + $2 \, mmol/l$ ferroin + $0.2 \, g/l$ Triton X-100 surfactant) are pumped into a beaker of volume $V_r = 15 \, ml$ at room temperature ($21 \, °C$). The reaction mixture is stirred at 800 rpm, and the volume is held constant by removing the excess reaction mixture using a suction pump; the reactor residence time is 800 s. A Pt electrode is immersed directly into the reaction mixture, and a Ag|AgCl|KCl electrode is connected to it through a junction holding saturated K_2SO_4 solution. The potential (E) between electrodes is measured using a pH meter connected to a PC through a

USB data acquisition board. The redox potential is monitored and recorded at a sampling rate of 2 Hz using a computer program, which also carries out the pulse-perturbations via solenoid valves that release small volumes ($V_p < 0.1 \, ml$) of the inhibitor stock solution ($[KBr]_{stock} = 10$–$200 \, mmol/l$ containing $0.25 \, mol/l \, H_2SO_4$). The instantaneous concentration of the added KBr is calculated as $[KBr] = [KBr]_{stock} V_p V_r^{-1}$.

III. RESULTS AND MODEL

The unperturbed ferroin-catalyzed BZ reaction exhibits strong relaxation-type oscillations with a relaxed period T_0 of $100 \pm 5 \, s$ and a waveform that resembles the action potentials of tonically active neurons. Upon perturbation with KBr, the next peak is delayed (inhibition) and the unperturbed cycles that follow are extended as well. The relaxed frequency ($\Omega = T_0^{-1}$) is recovered after the oscillator remains unperturbed for several cycles [Fig. 1(a)]. We tested the effects of multiple perturbations by perturbing consecutive cycles after a fixed delay (τ_p) following each peak. Figure 1(b) shows that the perturbations have a cumulative effect: the higher the number of perturbations, the greater the deviation from the relaxed frequency.

We capture this behavior using a simple two variable model

$$\frac{d\phi}{dt} = \omega - \delta(\phi - 1), \tag{1}$$

$$\frac{d\omega}{dt} = \frac{\Omega - \omega}{\tau_\omega}. \tag{2}$$

We define the phase as the time elapsed since the last peak normalized to the *relaxed* cycle length, $\phi = (t - t^*)/T_0 \mod 1$, where t and t^* are the time since the start of the experiment and time of the last peak, respectively. The phase advances at the instantaneous frequency ω and is reset to zero when ϕ reaches 1 [$\delta()$ is the Dirac delta function]; ω slowly relaxes to Ω with a time constant $\tau_\omega \gg \Omega^{-1}$.
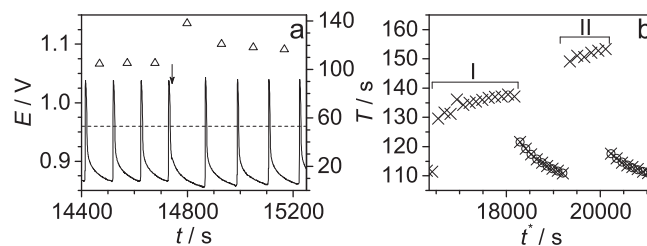
FIG. 1. Experimental data. (a) Electrochemical potential *vs.* time (solid line), peak detection threshold = 0.96 V (dashed line); period (T) *vs.* time (open triangles); arrow indicates a single perturbation with $[KBr] = 0.5 \, mmol/l$. (b) Cycle lengths *vs.* peak times (t^*) in repeated perturbation experiments with parameters listed as 2 (time span I) and 3 (time span II) in Table I. Crosses indicate periods in experiments; open circles show calculated values of unperturbed periods.

During any *unperturbed* time interval between peaks, $\phi(t)$ and $\omega(t)$ can be calculated by integrating Eqs. (1) and (2)

$$\phi(t) = \phi_0 + \Omega(t - t_0) + \tau_\omega(\Omega - \omega_0)(e^{-\frac{t-t_0}{\tau_\omega}} - 1), \quad (3)$$

$$\omega(t) = \Omega - (\Omega - \omega_0)e^{-\frac{t-t_0}{\tau_\omega}}. \quad (4)$$

From here on, ϕ and ω refer to the variables and $\phi(t)$ and $\omega(t)$ to the integrated forms.

In order to obtain τ_ω from the experimental data such as that shown in Fig. 1(b), we need to derive the explicit form of the cycle length of an oscillator with $\omega < \Omega$. We first obtain the inverse of Eq. (3); i.e., we solve for the time, t, as a function of the phase, ϕ,

$$t(\phi) = t_0 + \frac{\phi - \phi_0}{\Omega}$$
$$+ \tau_\omega \left\{ W \left[\left(\frac{\omega_0}{\Omega} - 1 \right) e^{\frac{1}{\Omega}\left(\omega_0 - \frac{\phi - \phi_0}{\tau_\omega} \right) - 1} \right] - \left(\frac{\omega_0}{\Omega} - 1 \right) \right\}, \quad (5)$$

where $W()$ is the Lambert W-function, defined by $z = W(ze^z)$. To make our notation cleaner, we define $\mathring{\phi}(t)$, $\mathring{\omega}(t)$, and $\mathring{t}(\phi)$ as the respective functions with initial parameters $\phi_0 = 0$ and $t_0 = 0$. We define the following function to calculate the *unperturbed* cycle length:

$$\Theta(\omega) = \mathring{t}(1|\omega_0 = \omega). \quad (6)$$

We find the period of the first cycle as $\Theta(\omega_0)$. To do the same for the second cycle, we first need to calculate the instantaneous frequency at the beginning of that cycle, $\omega[\Theta(\omega_0)]$. Then, we can use Eq. (6) again. For any cycle after the first one in a relaxation sequence, the period can be calculated as a composition of functions

$$f(x) = \Theta[\mathring{\omega}(t)], \quad (7)$$
$$T_n = f \circ f \circ \cdots \circ f[\Theta(\omega_0)]. \quad (8)$$

Since no perturbation occurs, all cycle lengths depend only on τ_ω and ω_0 for the first cycle.

We determined the model parameter τ_ω by fitting the calculated periods to the relaxation segments in T *vs.* time series similar to those shown in Fig. 1(b). In each such experiment, ω_0 of the first *unperturbed* cycle needed to be fitted as well, because ω is an unobserved variable. Although we measured Ω at the beginning of the experiments, the goodness of fit (measured by the F-test) was better when we fitted Ω as well. We used the L-BFGS-B algorithm[21] implemented in the R software package[22] to obtain the fits.

In Table I, we report the parameters of fits that had $p < 0.002$. Our experimental results do not show an obvious dependence of τ_ω on [KBr] or on the delay between peaks and perturbations (τ_p) preceding relaxation. The average (765 ± 57 s) of the results shown in Table I is close to the residence time of the reactor (800 s). Changing the threshold of p to 10^{-4} only slightly changes the value obtained. We use $\tau_\omega = 800$ s in our calculations.

TABLE I. Fitted parameters of frequency relaxation.

No.	[KBr] (M)	τ_p (s)[a]	τ_ω (s)	Ω^{-1} (s)	p
1.	2×10^{-5}	30	946.7	110.9	4×10^{-4}
2.	5×10^{-5}	10	567.1	108.2	4×10^{-8}
3.	5×10^{-5}	30	813.5	106.4	2×10^{-10}
4.	5×10^{-5}	60	689.9	108.2	1×10^{-6}
5.	5×10^{-5}	80	849.0	109.1	1×10^{-8}
6.	1×10^{-4}	10	899.9	108.4	4×10^{-10}
7.	1×10^{-4}	80	590.4	137.5	1×10^{-3}

[a]Delay between peaks and perturbations preceding relaxation.

Next, we extend our model by adding terms that describe the effect of perturbations

$$\frac{d\phi}{dt} = \omega - \delta(\phi - 1) + g(\varepsilon, \phi)\delta(t - t_p), \quad (9)$$

$$\frac{d\omega}{dt} = (\Omega - \omega)\tau_\omega^{-1} - \kappa(\varepsilon)\omega\delta(t - t_p). \quad (10)$$

Perturbations occurring at $t = t_p$ reset the phase according to the PRC, $g(\varepsilon, \phi)$, parameterized by the perturbation strength, ε, which is equal to [KBr] in our experiments. They also reduce the instantaneous frequency by $\kappa(\varepsilon)\omega$, where $\kappa(\varepsilon)$ is the perturbation strength-dependent frequency reduction constant.

We assume that $\kappa(\varepsilon)$ is independent of the phase of perturbation. Therefore, we can obtain $\kappa(\varepsilon)$ by fitting the relaxation segments in the PRC measurement period *vs.* time series [Fig. 2(a)]. Each such sequence starts with $\omega_0 = \Omega$. After the first perturbation $\omega = (1 - \kappa)\Omega$, followed by frequency relaxation until the next perturbation when it decreases further by $\kappa\omega$. In order to find κ, we fitted the periods calculated using Eq. (6) to the experimental periods using the least squares method. In Fig. 2(b), we report the κ values and a linear fit of $\kappa(\varepsilon)$ in the range of 1×10^{-5}M to 5×10^{-4}M. Note that at the highest perturbation strength, each perturbation was measured to decrease the instantaneous frequency by about 17%.

Besides the frequency change, oscillators experience phase reset when perturbed, which is calculated as $\Delta\phi = 1 - T/T_0$, where T is the length of the *perturbed* cycle. The magnitude of $\Delta\phi$ depends on both the phase of the perturbation and its strength ([KBr]). The phase reset as a function of the observed phase is referred to as the latent PRC. We measured the latent PRCs of the ferroin-catalyzed BZ oscillator at $[KBr] = 5 \times 10^{-6}$M to 5×10^{-4}M [Fig. 3(a)]. All PRC values are negative (phase delay), and the values decrease monotonically as ϕ and ε increase. PRCs at higher [KBr] exhibit values that no longer obey $\Delta\phi \geq -\phi$, which means that some perturbations reset the phase to negative values. Similar behavior was found in the Wang-Buzsáki neuron,[23] a model[24] commonly used in computational neuroscience.

We obtained the parameters required to calculate the relaxation dynamics; thus, it is possible to extract the true
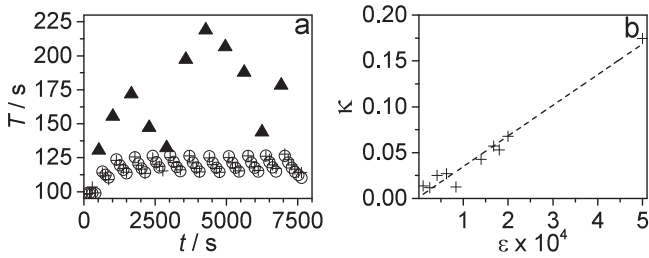
FIG. 2. (a) Periods *vs.* peak times during PRC measurement at [KBr] = 5 × 10⁻⁴M: periods of unperturbed cycles (crosses) and perturbed cycles (solid triangles), calculated periods of unperturbed cycles with the fitted κ and t_ω parameters (open circles). (b) Frequency reduction constant as a function of coupling strength. Experimental data (crosses) and linear fit $\kappa(\varepsilon) = 342.5 \times \varepsilon$ (dashed line).

PRCs from the experimental data. We first calculate the instantaneous frequencies at the beginning of the perturbed cycles and immediately after the perturbations. The same formula can be used to calculate how much the phase advances from the beginning of the cycle until a perturbation ($\Delta t_p = t_p - t^*$), and from the perturbation until the end of the perturbed cycle ($\Delta t_l = t_{end} - t_p$). The phase reset is then given by Eq. (11)

$$\Delta\phi = 1 - \{\mathring{\phi}(\Delta t_p | \omega_0) + \mathring{\phi}[\Delta t_l | (1 - \kappa)\mathring{\omega}(t_p)]\}. \quad (11)$$

PRCs corrected for the deviation from the relaxed cycle are shown in Fig. 3(a). They express the phase reset when an oscillator with relaxed frequency is perturbed with KBr. These possess two major differences compared to the latent PRCs: (1) $\Delta\phi$ is smaller and (2) their magnitudes reach a plateau at about $\varepsilon = 1.8 \times 10^{-4}$ as illustrated in Fig. 3(b) in the $\Delta\phi$ *vs.* ε plot at $\phi = 0.7388$.

To generate a family of PRC functions over a continuous range of ε, we used a functional form derived from the
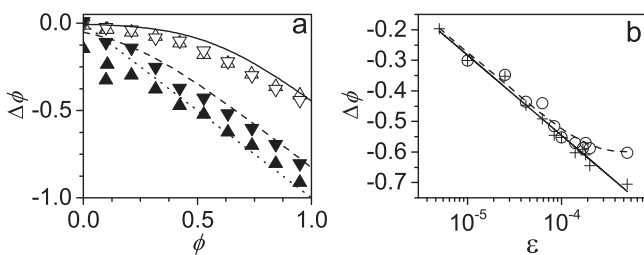
FIG. 3. (a) Experimentally determined latent inhibitory PRCs at [KBr] = 1 × 10⁻⁵M (open triangles) and [KBr] = 5 × 10⁻⁴M (solid triangles) (medians of 4 repetitions shown). PRCs corrected for frequency change (corresponding inverted symbols). PRCs calculated using Eq. (12) with parameters $T_0 = 100$s, $k = 6.235 \times 10^{-2}\,\text{s}^{-1}$, $\varepsilon_0 = 3.147 \times 10^{-4}$ and $\varepsilon = 1 \times 10^{-5}$ (solid line), and $\varepsilon = 5 \times 10^{-4}$ (dashed line). $\Delta\phi = -\phi$ (dotted line). (b) $\Delta\phi$ *vs.* ε at $\phi = 0.7388$ of latent PRCs (crosses) and corrected PRCs (open circles), trend of latent PRCs (solid line), approximate trend of corrected PRCs (dashed line).

chemical kinetics of the BZ reaction[25]

$$g(\varepsilon, \phi) = -\left[\phi + \frac{1}{kT_0} \ln\left(e^{-kT_0\phi} + \frac{\varepsilon}{\varepsilon_0}\right)\right]. \quad (12)$$

The constants k and ε_0 depend on the experimental control parameters (chemical composition, flow rate, etc.); T_0 is the relaxed cycle length. In order to match the corrected experimental PRCs, we set $T_0 = 100$ s, and we obtained the other two parameters by fitting Eq. (12) to the corrected PRCs in the concentration range of 1×10^{-5}M to 1.68×10^{-4}M (just before the corrected PRCs plateau). PRCs calculated using the fitted parameters are shown in Fig. 3(a). The maximum magnitude of the inhibitory PRCs is achieved at $\varepsilon = 1.68 \times 10^{-4}$; corrected PRCs at higher ε are identical.

The variable frequency has an important impact on the peak delays caused by perturbations: the lower the oscillator's frequency, the more the next peak is delayed by identical phase resets. The consumption of added KBr proceeds according to a pseudo-first order chemical reaction,[25] the rate constant of which depends only on the reagent concentrations of the BZ reaction, which are kept constant by the flow. Therefore, consuming the added KBr should take the same time, provided that the additions occur at the same phase. We need to ensure that this behavior is preserved in our model by rescaling the phase reset when $\omega < \Omega$.

Using Eq. (5), we can find the time it takes for the initially *relaxed* oscillator to advance the amount of phase given by the PRC when the frequency is reduced to $\omega_{0,r} = [1 - \kappa(\varepsilon)]\Omega$ by the perturbation. We then calculate the phase reset that causes an equivalent peak delay when the oscillator has been perturbed earlier $\{\omega_{0,p} = [1 - \kappa(\varepsilon)]\omega\}$ using Eq. (3). The rescaled phase reset with the composition of the PRC, Eqs. (3) and (5), and the frequencies of the *relaxed* and the *perturbed* oscillator immediately after perturbation are given by

$$h(\varepsilon, \phi, \omega) = -\mathring{\phi}\{\mathring{t}[-g(\varepsilon, \phi)|\omega_{0,r}]|\omega_{0,p}\}. \quad (13)$$

To model the behavior of two coupled oscillators, we used two pairs of the following generic equations:

$$\frac{d\phi_i}{dt} = \omega_i - \delta(\phi_i - 1) + h(\varepsilon_{j\to i}, \phi_i, \omega_i)\delta[\phi_j(t - \tau)], \quad (14)$$

$$\frac{d\omega_i}{dt} = \frac{\Omega_i - \omega_i}{\tau_{\omega_i}} - \kappa(\varepsilon_{j\to i}), \omega_i\delta[\phi_j(t - \tau)], \quad (15)$$

where $\varepsilon_{j\to i}$ is the coupling strength for the connection $j \to i$ and τ is an optional time delay between each peak of oscillator j and the ensuing perturbation to oscillator i.

IV. DISCUSSION

The model equations are uncoupled between peaks and perturbations, which allows for the use of the integrated formulas during these segments. Thus, solutions can be obtained by an event-based method.

Starting from random initial conditions (ϕ_1, ϕ_2) and oscillators at their natural frequencies, $\omega_{1,2}(t = 0) = \Omega_{1,2}$, we first use Eq. (5) to find the times (t_1^*, t_2^*) it takes for each oscillator to

reach $\phi = 1$. The first firing occurs (t^*) at $\min(t_1^*, t_2^*)$, which sets the window of this iteration. We set the phase of the oscillator that fires first to zero and calculate the phase of the other oscillator using Eq. (3). We must also calculate the frequency of each oscillator at (t^*). Then, we can calculate the effect of the perturbation on the oscillator that did not fire. We set its phase and reduce its frequency according to Eq. (13) and $\omega_r = [1 - \kappa(\varepsilon)] \omega$, respectively. This completes the first iteration, the results of which are used as initial conditions for the second iteration. This procedure allows us to find the peaks and perturbations when the coupling is instantaneous ($\tau = 0$).

When there is a delay between peaks and perturbations ($\tau > 0$), we need to maintain a list of upcoming perturbations, where each element contains the time of the perturbation, the target oscillator, and the strength of the perturbation. Thus, the previous procedure must be modified slightly: at the beginning, when the times of the next firings are calculated, we must check whether a peak or a perturbation occurs first. If a peak occurs first, we proceed according to the procedure above. If a perturbation occurs first, we set the time window to the time of the next perturbation (t_p). Then, we calculate the phases and frequencies of the oscillators using Eqs. (3) and (4) at t_p. We perform the delayed perturbation on the target oscillator: we reset the phase and reduce the frequency as described above. Finally, we remove the perturbation from the perturbation array and start the next iteration with the results of the current iteration used as initial conditions.

We implemented an algorithm based on this approach in MATLAB[26] and calculated the time series for a large matrix of coupling strength pairs. In Fig. 4, we show domains of the simulated behaviors in the $\varepsilon_{1 \to 2}$ vs. $\varepsilon_{2 \to 1}$ phase plane. Our model is able to simulate the behaviors displayed by two pulse-coupled BZ oscillators with unequal inhibitory coupling.[20] The calculated patterns appear in the correct coupling strength ranges when we use parameters extracted from experiments with a single pulse-perturbed oscillator. The 1:N and OS patterns predominate [Fig. 4(a)], when there is no time delay between peaks and perturbations ($\tau = 0$). When $0 < \tau < T_0/2$, the N:M type patterns are also reproduced [Fig. 4(b)].
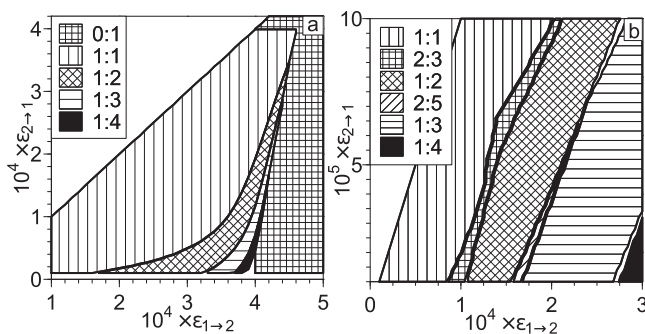
FIG. 4. Calculated map of behaviors for the asymmetric coupling arrangement where $\varepsilon_{1 \to 2} \geq \varepsilon_{2 \to 1}$, $\tau_\omega = 800$, $\Omega_1 = \Omega_2 = 0.01$, $\tau = 0$ (a), $\tau = 7$ (b), $\phi_1^0 = 0.7$, $\phi_2^0 = 0.2$.

Our approach is similar to the phase-amplitude description of neural oscillator models by Wedgwood et al.;[27] however, the amplitude is not a reliable observable in our system, which would hinder our attempts to extract model parameters from our experimental data by fitting. Our approach requires that the long-term dynamics of the frequency follow a simple exponential decay with a decay-constant (τ_ω) that is independent of the history of the system. More complex long-term dynamics (e.g., multiple processes affecting the frequency, or decay of higher order) will require extensive modifications, potentially limiting the derivation and the use of closed form solutions. While our method assumes that the frequency of the oscillator is reduced after a strong perturbation, it is straightforward to modify it to capture frequency increase as a result of a perturbation.[18]

V. CONCLUSIONS

The description of dynamics using our model does not assume in-depth knowledge of the underlying chemistry of the system. The functions derived specifically from the chemistry of the BZ oscillator can be replaced by functional approximations. This method may straightforwardly be adapted to model the dynamics of systems (e.g., networks of neurons), where the coupling is strong and interactions cause the dynamics of the oscillators to undergo long-term changes. Since these equations can be solved on the basis of events, larger scale systems, which have been of interest in physics and computational neuroscience, can be easily explored.

REFERENCES

[1] J. Maselko, J. S. Reckley, and K. Showalter, J. Phys. Chem. **93**, 2774 (1989).
[2] A. F. Taylor, M. R. Tinsley, F. Wang, Z. Huang, and K. Showalter, Science **323**, 614 (2009).
[3] A. F. Taylor, M. R. Tinsley, F. Wang, and K. Showalter, Angew. Chem. Int. Ed. **50**, 10161 (2011).
[4] J. F. Totz, J. Rode, M. R. Tinsley, K. Showalter, and H. Engel, Nat. Phys. **14**, 282 (2018).
[5] E. R. Kandel, J. H. Schwartz, and T. M. Jessell, *Principles of Neural Science*, 4th ed. (McGraw-Hill, New York, 2000).
[6] C. C. Canavier and S. Achuthan, Math. Biosci. **226**, 77 (2010).
[7] R. E. Mirollo and S. H. Strogatz, SIAM J. Appl. Math. **50**, 1645 (1990).
[8] U. Ernst, K. Pawelzik, and T. Geisel, Phys. Rev. Lett. **74**, 1570 (1995).
[9] M. Zeitler, A. Daffertshofer, and C. C. A. M. Gielen, Phys. Rev. E **79**, 065203(R) (2009).
[10] E. M. Izhikevich, *Dynamical Systems in Neuroscience: The Geometry of Excitability and Bursting* (MIT Press, Cambridge, 2007).
[11] G. B. Ermentrout and N. Kopell, SIAM J. Appl. Math. **50**, 125 (1990).
[12] M. I. Rabinovich, P. Varona, A. I. Selverston, and H. D. I. Abarbanel, Rev. Mod. Phys. **78**, 1213 (2006).
[13] M. Oh and V. Matveev, J. Comput. Neurosci. **26**, 303 (2009).
[14] A. Winfree, J. Theor. Biol. **16**, 15 (1967).
[15] Y. Kuramoto, *Chemical Oscillations, Waves and Turbulence* (Springer, Berlin, 1984).

[16] H. Haken, *Brain Dynamics* (Springer, New York, 2008).

[17] I. Z. Kiss, Y. M. Zhai, and J. L. Hudson, Phys. Rev. Lett. **94**, 248301 (2005).

[18] J. X. Cui, C. C. Canavier, and R. J. Butera, J. Neurophysiol. **102**, 387 (2009).

[19] M. R. Guevara, A. Shrier, and L. Glass, Am. J. Physiol. **251**, H1298 (1986).

[20] V. Horváth, D. J. Kutner, J. T. Chavis III, and I. R. Epstein, Phys. Chem. Chem. Phys. **17**, 4664 (2015).

[21] R. H. Byrd, P. Lu, J. Nocedal, and C. Zhu, SIAM J. Sci. Comput. **16**, 1190 (1995).

[22] R Core Team, R: A *Language and Environment for Statistical Computing* (R Foundation for Statistical Computing, Vienna, Austria, 2016).

[23] M. Oh and V. Matveev, J. Comput. Neurosci. **31**, 31 (2011).

[24] X. J. Wang and G. Buzsáki, J. Neurosci. **16**, 6402 (1996).

[25] P. Ruoff, J. Phys. Chem. **88**, 2851 (1984).

[26] MATLAB, version 8.3.0.532 (R2014a), The MathWorks Inc., Natick, MA, 2014.

[27] K. C. A. Wedgwood, K. K. Lin, R. Thul, and S. Coombes, J. Math. Neurosci. **3**, 2 (2013).